Colloid Polym Sci (2009) 287:147–155
DOI 10.1007/s00396-008-1958-z

ORIGINAL CONTRIBUTION

Crystallization behavior and hydrophilicity of poly(vinylidene fluoride) (PVDF)/poly(methylmethacrylate) (PMMA)/poly(styrene-*co*-acrylonitrile) (SAN) ternary blends

Wenzhong Ma · Shuangjun Chen · Jun Zhang · Xiaolin Wang

Received: 17 August 2008 / Revised: 9 October 2008 / Accepted: 21 October 2008 / Published online: 8 November 2008

Abstract Compatibilization of the partially miscible poly (vinylidene fluoride) (PVDF)/poly(styrene-*co*-acrylonitrile) (SAN) pair by a third homopolymer, i.e., poly(methyl methacrylate) (PMMA), was investigated in relation to cross section morphology, crystallization behaviors and hydrophilicity of the polyblends. Scanning electron microscopy showed a more regular and homogeneous morphology when more than 15 wt.% PMMA was incorporated. The samples presented only α phase regardless of PMMA content in the blend. As the PMMA content increased in the blends, the interactions between each component were enhanced, and the crystallization of PVDF was limited, leading to a decreasing of the crystallinity and the crystallite thickness. Besides, the hydrophilicity of PVDF was further improved by PMMA addition. The sample containing 15 wt.% PMMA showed a more hydrophilic property due to the more polar part of surface tension induced by PMMA addition. Observed from the cross section of the blends, the miscibility of partially miscible PVDF/SAN blends were efficiently improved by PMMA incorporation.

W. Ma · S. Chen · J. Zhang (✉)
College of Materials Science and Engineering,
Nanjing University of Technology,
Nanjing 210009, China
e-mail: zhangjun@njut.edu.cn

X. Wang
Department of Chemical Engineering, Tsinghua University,
Beijing 100084, China

Keywords Ternary blends · Crystallization · Hydrophilicity · Miscibility · Poly(vinylidene fluoride) (PVDF) · Poly(methyl methacrylate) (PMMA) · Poly(styrene-*co*-acrylonitrile) (SAN)

Introduction

Polymer blends play an important role in the preparing of new high performance polymeric materials for special applications. This method is a versatile, straightforward, and relatively inexpensive one for modifying the properties of polymer materials and has attracted tremendous attention over the past decades. From an exclusively thermodynamic point of view, the blends may be classified as miscible, partially miscible, and immiscible systems [1]. Current theory to identify the miscibility the blend mainly uses the concentration dependences of the glass transition and depression of the melting point [2, 3]. The blends presenting a single T_g criterion is possible to be considered as miscible. With regard to the blend containing crystallizable component, the thermodynamic interactions in the blends is described by melting point depression. Recently, there have been numerous reports of miscibility, crystallization, and melting behavior of binary blends of poly (vinylidene) fluoride (PVDF)/amorphous polymer, including PVDF/ poly (methyl methacrylate) (PMMA) [2], PVDF/ poly (vinyl fluoride) (PVF) [4], PVDF/poly(vinyl acetate) (PVAc) [5], PVDF/poly(vinylpyrrolidone) (PVP) [6], PVDF/poly(3-hydroxybutyrate) (PHB) [7] and etc. It has been demonstrated that PVDF could be miscible with oxygen-containing polymers which is related to the

interaction between the fluorine atoms and carbonyl groups of the partner polymer [8]. However, as reported in Li's work [9], not all carbonyl-group-containing polymers are miscible with PVDF. They found that PVDF can be miscible with poly(trimethylene adipate) (PTA) (with a CH_2/CO ratio of 3.5) and poly(pentamethylene adipate) (PPA) (with a CH_2/CO ratio of 4.5).

PVDF as a semi-crystalline polymer with excellent physical and chemical properties, as well as good thermal stability, has been widely used in many applications. However, because of its hydrophobic nature, PVDF's wide application in membranes process has been limited. In order to obtain more hydrophilic PVDF blends, PVDF/PMMA [10], and PVDF/polyacrylonitrile (PAN) [11] blends were applied to the membrane preparations. In the result, their hydrophilicity was enhanced and flux rate of the PVDF blend membrane increased by those hydrophilic materials. Among the publications about PVDF blends, few works focused on the ternary system. In Moussaif's work, the immiscible blend PVDF/PC was compatibilized by PMMA addition [12]. In this ternary blend, the more regular and finer phase dispersion, and better mechanical properties were presented. As far as the thermodynamic properties are concerned, the ternary blend system PVDF/PMMA/PVAc is miscible [13]. Kim et al. use poly(methyl methacrylate-*co*-methacrylic acid) (P(MMA-*co*-MAA)) of low methacrylic acid content as the compatibilizer to add into PVDF/nylon 6 blends [14]. It reveals that the compatibility and the energy of rupture in tensile testing for nylon 6 and PVDF is enhanced by adding P(MMA-*co*-MAA). Therefore, a substantial compatibilization upon the incorporation of a third polymeric component plays an important role in improving the miscibility and physical properties of the immisicible or partially miscible binary blends.

As reported in our previous work [15, 16], the hydrophilicity of PVDF can be improved by random incorporation of hydrophilic polymer (PMMA, SAN) into the PVDF matrices. In the whole range of PMMA composition, PVDF/PMMA blend system has a good miscibility. However, the binary blend of PVDF/SAN is a partially miscible system as the PVDF content is higher than 50 wt.%. As demonstrated in our previous work [15], when PVDF is rich in the binary blend (PVDF/SAN), the one with 70 wt.% PVDF maintains the original properties of PVDF and shows better hydrophilicity, but this system is not miscible. The low miscibility would lead to gross phase separation and poor interfacial adhesion [12]. Therefore, in order to prepare more hydrophilic PVDF/SAN (with 70 wt.% PVDF) blend which maintains good properties of PVDF and SAN component, the miscibility should be improved. As known, PMMA and SAN have the miscibility due to intramolecular repulsive forces in the SAN component [17]. Thus, in this work, in order to improve the miscibility, PMMA, which was considered as a compatibilizer, was incorporated into PVDF/SAN blend. The effect of PMMA composition on the miscibility, morphology, and hydrophilicity of PVDF/SAN blend was investigated.

Experimental

Materials

PVDF (Kynar K-761, $\overline{M}w = 441,000$) was supplied by Elf Atochem of North America Inc. (USA). PMMA (HR1000L) was obtained from Kuraray Co., Ltd (Japan). SAN (D-178, in which the acrylonitrile content is 26 wt.%) was purchased from Zhenjiang Guoheng Chemical Limited Company (China).

Melt blending and specimen preparation

The melt blending of PVDF/PMMA/SAN was carried out with a torque rheogoniometer (Kechuang Machinery XSS-300, China) at 180 °C and 60 rpm for 10 min. A set of the blends with weight fractions of PVDF/PMMA/SAN containing 70/0/30, 70/9/21, 70/15/15, 70/21/9, and 70/30/0 (*w*/*w*) were prepared. Then, the blend samples were prepared by compression molding at 180 °C with the platen vulcanizing press (5 MPa) for 10 min, and then cooled at room temperature still under pressure (10 MPa). Thus, the flat sheet samples (about 0.5 mm) possessing smooth surfaces were obtained. Subsequently, the series of measurements were performed.

Scanning electron microscopy (SEM) observation

The samples were fractured in liquid nitrogen, and the surfaces were sputtered with Pt in vacuum. Then, the SEM micrographs of dried and gold-coated cross sections were taken with a JEOL JSM-5900 instrument.

Fourier transform infrared spectroscopy (FTIR) measurement

Fourier transform infrared spectroscopy (FTIR) spectra were obtained by a Bruker IFS 66/s with 4 cm^{-1} resolution. FIIR-attenuated total reflection (ATR) spectra were applied in this work.

Wide-angle X-ray diffraction measurement

Wide-angle X-ray diffraction (WAXD) was done with a Shimadzu XRD-6000 diffractometer (Cu K_α radiation,

40 kV and 30 mA). The scanning angle ranged from 5°~50° with the scanning velocity of 4°/min. The interplanar distance (d-value) and the crystallite thickness L was calculated using the Bragg equation and Scherrer equation [18], respectively, as our previous work [16, 19].

Differential scanning calorimetry (DSC)

The calorimetric measurements were made on a TA Instruments Q-200 differential scanning calorimeter in a dry nitrogen atmosphere. In order to erase the thermal history of the samples, the polymer blend samples (ca. 10 mg) were heated from room temperature to 180 °C at a rate of 40 °C/min. Maintained at 180 °C for 5 min, the mixtures were cooled down to 40 °C at a rate of 5 °C/min (the cooling run). After 1 min at 40 °C, a second heating was done upon to 180 °C. The glass transition temperature (T_g) was taken at the inflection point on the thermograms.

The crystallinity of PVDF (X_c) was recorded below, as our previous work [20, 21].

$$X_c = \frac{\Delta H_f / \phi}{\Delta H_f^*} \times 100\%$$

Where $\Delta H_f^* = 104.5 \mathrm{J/g}$ [22] is the melting enthalpy for a 100% crystalline PVDF, ΔH_f is the melting enthalpy of the mixtures measured in DSC, and ϕ is the weight fraction of PVDF in the blend (70 wt.%).

The crystallization half time ($t_{1/2}$), which is defined as the half time of crystallization [23], was used as a characteristic parameter of the crystallization process.

Contact angle test

The measurement of the contact angle of samples was carried out using a Krüss DSA-100 goniometer at 20 °C. Water and diiodomethane were used as the test liquids. The detailed procedure was the same as our previous work [16]. Then, the total solid surface tension γ_s, and its dispersive and polar component γ_s^d, γ_s^p were calculated by the Owens and Wendt method [24, 25].

Results and discussion

The miscibility of SAN with PVDF

SAN is a hydrophilic polymer material because of its nitrile group (–CN) [11], but just partially compatible with PVDF [15]. This kind of polymer blend will limit its application because of microheterogeneity and small interfacial adhesion. In order to overcome these shortcomings, PVDF/SAN blend should be compatibilized. As is known, PMMA, which has similar physical properties to SAN, is an amorphous and hydrophilic polymer material. As reported, PMMA is miscible with PVDF over the whole range of composition [16, 26–28]. On the other hand, PMMA and SAN have the miscibility due to intramolecular repulsive forces in the SAN component [17]. So PMMA can be used as the compatibilizer of the PVDF/SAN system. As expected, the compatibility of PVDF/SAN blend can be improved by adding with PMMA.

The PMMA component dependence of cross section morphology in PVDF/SAN blends with 70 wt.% PVDF is shown in Fig. 1. The PVDF/SAN (70/30) blend shows a typical morphology of partially compatible polymers, with small dispersed domains of SAN (Fig. 1a). In a ternary system (PVDF/PMMA/SAN; the fraction of PVDF is fixed at 70 wt.%), the increase of PMMA content makes the blend more homogeneous. Therefore, it is obviously observed that an incorporation of PMMA can efficiently improve the compatibility of PVDF/SAN blend. When only PMMA is blended with PVDF, the homogeneous morphology is obtained. This can be confirmed that PVDF/PMMA blend has high compatibility, as illustrated in our previous work [16].

IR spectroscopy

Figure 2 shows the IR spectra (in ATR mode) of the neat PVDF, neat PMMA, and ternary blends (PVDF/PMMA/SAN) with different weight fraction of each component. The samples containing PVDF have the well-defined absorption bands at 1,423, 1,400, 1,383, 1,210, 1,177, 1,068, 975, 870, 855, 794, 761, and 614 $\mathrm{cm^{-1}}$. As reported, these IR absorption bands represent the characteristic spectrum of the α phase of PVDF crystal [29, 30]. It indicates that the only crystallization of α phase PVDF predominates in the crystallization from the melt, which agrees with Gregorio's results [31]. It can be seen that the intensity of the characteristic α phase bands are not changed. This suggests that the crystalline phase of PVDF is not influenced by the change of the various ratios of PMMA and SAN content, when PVDF content is fixed at 70 wt.%. As for the neat SAN sample, the bands at 759 $\mathrm{cm^{-1}}$ and at 699 $\mathrm{cm^{-1}}$ show the presence of the out-of-plane hydrogen vibration for styrene co-polymer [32]. As PVDF blended with SAN, the band at 759 $\mathrm{cm^{-1}}$ is overlapped by the more intensive α phase PVDF band (761 $\mathrm{cm^{-1}}$).

In addition, when PMMA blended with PVDF or PVDF/SAN blend, the band at 1,722 $\mathrm{cm^{-1}}$, which refers to the carbonyl band in PMMA component, is enhanced and shifts to a higher wavenumber. The enhancing of this band

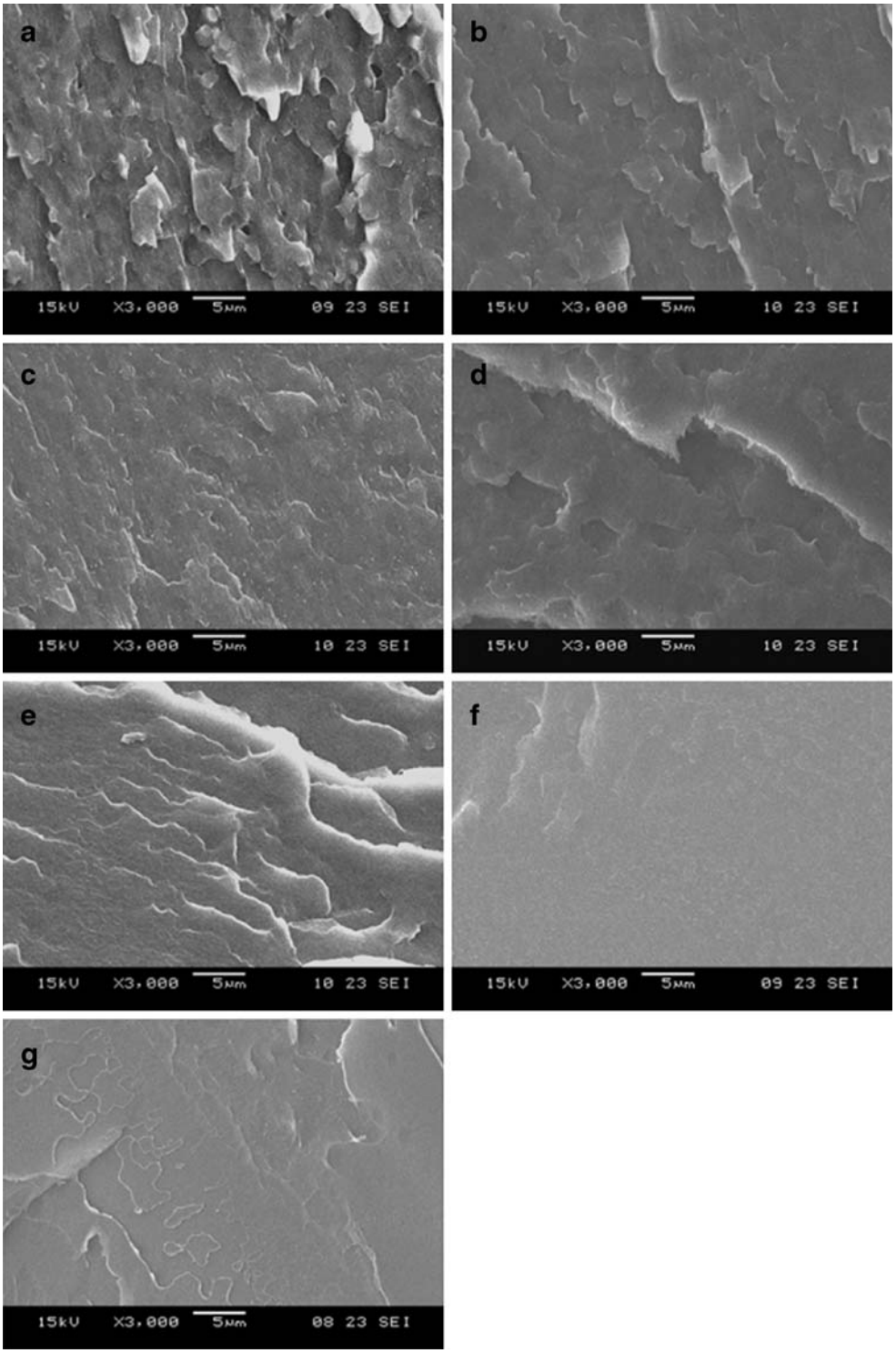

Fig. 1 SEM micrograph of cross section of PVDF/PMMA/SAN blends with various mass ratios: **a** 70/0/30; **b** 70/9/21; **c** 70/15/15; **d** 70/21/9; **e** 70/30/0; **f)** neat SAN; **g** neat PMMA

is due to the increased PMMA content in the blend. The small shift of the carbonyl band indicates the occurrence of weak interactions between C=O and $–CF_2$ groups [33]. It imparts a high miscibility to PVDF/PMMA system. So PMMA is selected to improve the miscibility of PVDF/SAN blend.

WAXD analysis

X-ray diffractograms of the ternary blends and neat polymers are shown in Fig. 3. According to the researchers' work [30, 34, 35], the peaks at 2θ=18.05, 18.70, 20.27, 26.90, 33.37, 36.17, 37.43, and 39.00° in the curve for the

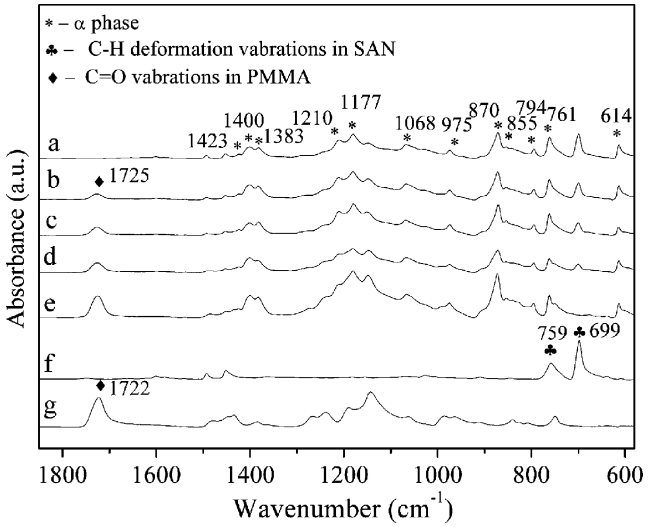

Fig. 2 IR spectra of PVDF/PMMA/SAN blends with various mass ratios: **a** 70/0/30; **b** 70/9/21; **c** 70/15/15; **d** 70/21/9; **e** 70/30/0; **f** neat SAN; **g** neat PMMA

neat PVDF sample (Fig. 3a), represent the diffractions in planes (100), (020), (110), (021), (130), (200), (210), and (002), respectively, which are all characteristic of the α phase of PVDF. It is noted that the values of the diffraction peak obtained in this work are a little higher than those obtained in the reference [30, 34]. This can be attributed to the difference in types of the apparatus which used for WAXD measurement. It is verified that all samples by melt

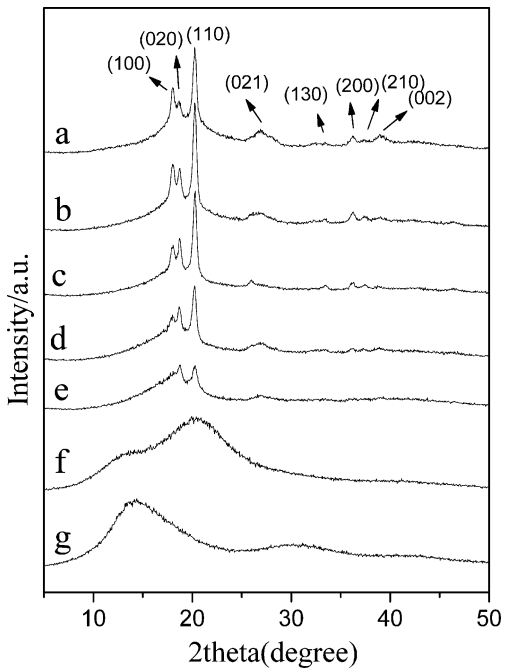

Fig. 3 X-ray diffractograms of PVDF/PMMA/SAN blends with various mass ratios: **a** 70/0/30; **b** 70/9/21; **c** 70/15/15; **d** 70/21/9; **e** 70/30/0; **f** neat SAN; **g** neat PMMA

molding, despite the various ratios of PMMA and SAN weight fraction in the blend, presents predominantly the α phase. All these peaks have a decrease in their intensity, as the PMMA composition increased in the blend, especially for the one at $2\theta=18.0°$, the decrease is the most remarkable as PMMA content increased. When only PMMA blended with PVDF, the peak at $2\theta=18.0°$ disappears. This suggests that the existence of PMMA in the blend significantly retards the growth of PVDF lamellae, which is due to the enhanced interactions between PVDF and other two polymer chains. As shown in Fig. 3, the ration of the intensities of the reflections assigned to (100) and (020) change dramatically. This possibly is due to the different limits to the growth of the PVDF lamella. As PMMA is incorporated into PVDF/SAN blend, the lamella L_{100} is affected remarkably, leading to obvious decrease in the intensities of the reflections (100). It has demonstrated that the crystallinity of a crystalline polymer can be related to the total scattering height of the peak in the WAXD [36]. Therefore, the crystallinity of PVDF in the blends is strongly affected by the increased PMMA content. As the mass ratio of PMMA/SAN is 30/0 in the blend, only two weak peaks at $2\theta=18.7$, 20.2° are illustrated, and other peaks disappear (Fig. 3e); i.e., the PVDF crystals are reduced more at this composition. With regard to the neat SAN178, PMMA samples, the amorphous humps instead of diffraction peaks are observed.

Table 1 lists the values of 2θ, interplanar spacing d, according to the three strong peaks observed in the diffractograms of Fig. 3. The crystallite thickness L_{hkl} in the direction perpendicular to the (hkl) crystal plane is calculated by Bragg equation and Scherrer equation [18], as

Table 1 WAXD data of ternary blends containing PVDF, SAN and PMMA

hkl	PVDF/PMMA/SAN blends	2θ (°)	*d* (Å)	*L* (Å)
100	70/0/30	18.05	4.91	119.0
	70/9/21	18.00	4.92	137.9
	70/15/15	18.05	4.91	109.6
	70/21/9	18.00	4.91	38.9
	70/30/0	–	–	–
020	70/0/30	18.65	4.75	–
	70/9/21	18.70	4.74	135.3
	70/15/15	18.70	4.74	153.8
	70/21/9	18.70	4.74	106.9
	70/30/0	18.70	4.74	102.0
110	70/0/30	20.22	4.39	183.1
	70/9/21	20.24	4.38	177.4
	70/15/15	20.24	4.38	179.3
	70/21/9	20.17	4.40	138.1
	70/30/0	20.22	4.39	150.0

– Not observed, θ Bragg angle, d the interplanar distance, L the crystallite thickness (1 Å=10^{-10} m)

reported in previous work [16, 37]. As shown in Table 1, the value d of all planes has nearly no change with different mass ratios of PMMA and SAN in the blends; i.e., the lattices parameter of the α phase is not affected. The values $L_{(100)}$, $L_{(020)}$ become larger when 9 wt.% PMMA added into PVDF/SAN blend, in comparison with the binary blend of PVDF/SAN (70/30). As demonstrated [16, 37], the miscible binary blend system, such as PVDF/PMMA and PEO/PMMA, the non-crystalline polymer molecules can be sandwiched in interlamellar regions. Therefore, the increased value L could be due to the trapped PMMA chains in the PVDF interlamellae. This confirms that less (9 wt.%) PMMA addition into the binary PVDF/SAN blend can improve their miscibility and favors the growth of PVDF lamellae. However, more presence of PMMA domains will induce some kind of perturbation which hinders the lamellar growth of PVDF in the blends. As detailed in Table 1, when PMMA content increases more (>9 wt.%), the crystallite thickness of PVDF becomes smaller. This result is well in agreement with our previous work [16]. It has been demonstrated that the less PMMA addition (<10 wt.%) into PVDF would favors the lamellae growth in the blend, leading to larger crystallite size. When more PMMA incorporated into PVDF, the growth of PVDF lamellae is reduced. In this work, similar result is obtained. When 9 wt.% PMMA is added into PVDF/SAN blend, the PVDF lamellae growth is favored, while, 15 wt.% or more PMMA incorporation will reduce the lamellae growth of PVDF (especially for $L_{(100)}$ and $L_{(020)}$). As for the crystallite thickness L_{110}, the small PMMA addition does not favor this lamella growth. The value L_{110} changes a little when the PMMA content is less than 15 wt.%, and it decreases more when more PMMA added. This means that the crystallite thickness L_{110} is decreased with PMMA addition.

Thermal properties and crystallinity

Figure 4 shows the DSC crystallization curves of neat polymer and blend samples during cooling from the melt at 5 °C/min after removing the thermal history. It is obviously observed that all the PMMA addition induce a significant decrease in the exothermic peak temperature, comparing with the PVDF/SAN (70/30) blend in which no PMMA added. In polymer/diluent system, the addition of diluent lowers the chemical potential of the mixture, leading to the depression of the crystallization temperature of PVDF diversely [38, 39]. Herein, as PMMA is incorporated into PVDF/SAN (70/30) blend, the dilution effect is enhanced. Therefore, the crystallization of PVDF is influenced more in these samples. This confirms that the interaction between each component of the ternary blend is enhanced by PMMA addition.

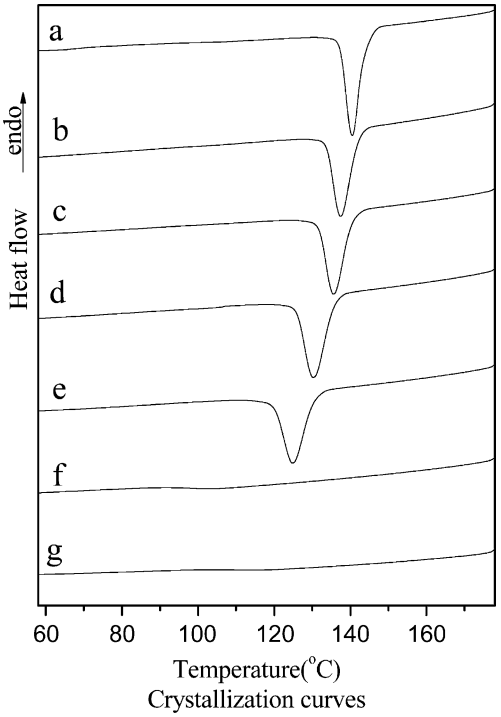

Fig. 4 DSC scans showing the crystallization traces of PVDF/PMMA/SAN blends with various mass ratios: **a** 70/0/30; **b** 70/9/21; **c** 70/15/15; **d** 70/21/9; **e** 70/30/0; **f** neat SAN; **g** neat PMMA

The data of the DSC crystallization results from Fig. 4 are summarized in Table 2. The crystallization temperatures and the value ΔH_c (enthalpy of crystallization) for PVDF in the blends depend upon various mass ratios of PMMA and SAN. The onset crystallization temperature T_c^{on}, peak crystallization temperature T_c^p, and final crystallization temperature T_c^f are decreased with an increase of PMMA addition in the ternary blends. The difference between the onset and peak crystallization temperature ΔT_c obtained from each sample is listed in Table 2. Beck [40] suggested

Table 2 DSC crystallization results of ternary blends containing PVDF, SAN and PMMA

samples	T_c^{on}	T_c^p	T_c^f	ΔT_c	ΔH_c	$t_{1/2}$
	°C	°C	°C	°C	J·g^{-1}	Min
PVDF/PMMA/SAN blends						
70/0/30	143.9	140.6	144.5	3.3	27.06	0.55
70/9/21	142.1	137.5	142.2	4.6	27.33	0.60
70/15/15	140.5	135.7	140.5	4.8	26.45	0.65
70/21/9	135.8	130.4	136.1	5.4	27.57	0.74
70/30/0	130.5	124.9	130.9	5.6	27.9	0.75
SAN178	–	–	–	–	–	–
PMMA	–	–	–	–	–	–

T_c^{on}: onset crystallization temperature of PVDF; T_c^p: peak crystallization temperature of PVDF; T_c^f: final crystallization temperature of PVDF; $\Delta T_c = T_c^{on} - T_c^p$; ΔH_c: crystallization enthalpy of PVDF.

that the small the values ΔT_c, the faster the overall crystallization rate, because the free expansion of crystals occurs between the onset and peak crystallization temperature [38]. It is shown that ΔT_c is increased with an increase of PMMA content in the ternary blends. This indicates that the PMMA content in the ternary blends has more disturbances on the crystallization of PVDF, and this influence is enhanced as the PMMA content increased. As reported [41, 42], the value $t_{1/2}$ is another parameter which characterizes the crystallization rate of polymer. The smaller the value $t_{1/2}$, the faster the crystallization rate, and vice versa. In Table 2, the value $t_{1/2}$ is increased with PMMA addition in the ternary blend. Therefore, the increased value $t_{1/2}$ and ΔT_c in the ternary blends suggests that the crystallization rate of PVDF is reduced by PMMA addition. It indicates that the interactions between PVDF and SAN chains can be improved by PMMA addition, leading to better compatibility of the ternary blend. In addition, among these ternary blends, the value ΔT_c of each sample has nearly no changes. This is due to the same weight fraction of PVDF in each sample.

Figure 5 shows the melting curves of PVDF, PMMA, SAN, and their blend samples after cooling from the melt. The evidence of a glass transition of the samples, as indicated in the melting curve can be observed in SAN, PMMA, and the blends containing SAN constituent. This glass transition phenomenon in the blends can be attributed to the amorphous domains. In the blend samples, the glass transition is broadened when PMMA content is increased. As only PMMA blended with PVDF (PVDF/PMMA=70/30), the glass transition is not visible in the melting trace. As detailed in Table 3, when PMMA is incorporated into PVDF/SAN blend, the value T_g of the blend is increased with an increase of PMMA addition. The change value of T_g indicates the enhanced interactions between the polymer chains in the blends.

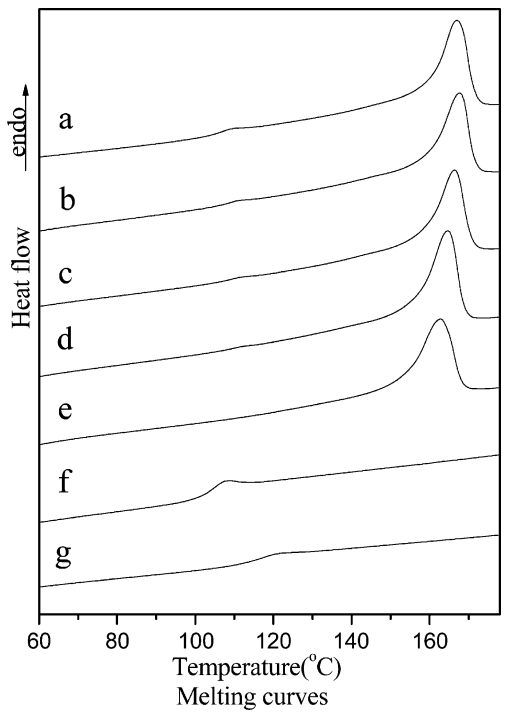

Fig. 5 DSC scans showing the melting traces of PVDF/PMMA/SAN blends with various mass ratios: **a** 70/0/30; **b** 70/9/21; **c** 70/15/15; **d** 70/21/9; **e** 70/30/0; **f** neat SAN; **g** neat PMMA

The presence of the glass transition can be explained by the distinctly different local segmental mobilities in the blend [43]. As our previous work [15], PVDF/SAN (70/30) is a partially miscible system. So, a microheterogeneity in this blend occurs in the sample (Fig. 1a). As proposed in the work of Kumar's group [43], even for the miscible blends, the molecular origins of the two different "dynamic microenvironments" (one with mobility approximately equal to the average blend mobility and the other close to the fast component) in systems with interactions and with T_g contrast. Herein, the two different microenvironments should be the rich PVDF phase and the additional amorphous polymer phase (SAN or SAN/PMMA), leading to the melting of PVDF crystals and glass transition in the melting traces.

Additionally, in Fig. 5, the melting peak is decreased with an increase of PMMA addition. As reported [2, 26], depression of melting points, due to a decrease in the chemical potential of the crystalline polymer, can provide the information on miscibility and strength of intermolecular interactions in the mixture. The higher depth of melting point depression occurs, the stronger interaction between the components of the mixture exists. So, it is suggested that the interaction between the PVDF, PMMA, and SAN chains can be enhanced by an increase of PMMA addition.

Table 3 DSC melting results of ternary blends containing PVDF, SAN and PMMA

Samples	T_g	T_m^{on}	T_m^p	T_m^f	ΔT_m	ΔH_m	X_c
	°C	°C	°C	°C	°C	J·g^{-1}	%
PVDF/PMMA/SAN blends							
70/0/30	105.4	159.1	166.9	171.8	12.7	28.08	38.4
70/9/21	108.9	159.0	167.6	171.8	12.8	26.98	36.9
70/15/15	110.3	157.9	166.3	170.8	12.9	27.0	36.9
70/21/9	111.8	156.0	164.5	169.6	13.6	26.42	36.1
70/30/0	–	152.7	162.7	168.2	15.5	26.39	36.1
SAN	104.2	–	–	–	–	–	–
PMMA	116.2	–	–	–	–	–	–

T_m^{on} Onset melting temperature of PVDF, T_m^p peak melting temperature of PVDF, T_m^f final melting temperature of PVDF, $\Delta T_m = T_m^f - T_m^{on}$ ΔH_m melting enthalpy, X_c crystallinity of PVDF

Table 3 lists the data obtained from the melting curves in Fig. 5, and summarizes the influence of the PMMA/SAN mass ratio in the ternary blend on PVDF crystallization during the heating. The onset of melting temperatures $\left(T_m^{on}\right)$, the peak melting temperature $\left(T_m^{p}\right)$, and the final melting temperatures $\left(T_m^{f}\right)$ of the PVDF blend samples are decreased with an increase of PMMA addition. This suggests the increased interaction between PVDF, PMMA, and SAN chains when PMMA was added. The difference in value ΔT_m $\left(\Delta T_m = T_m^{f} - T_m^{on}\right)$ indicates the formation of different PVDF crystal size. The higher the value of ΔT_m, the less homogeneity of PVDF crystal size. Therefore, the influence on crystallization of PVDF in the ternary blend is enhanced by PMMA addition.

The value ΔH_m (proportional to the crystallinity of the blends) for the ternary blend with PMMA addition is smaller than that for PVDF/SAN (70/30) sample. This implies that the crystallinity of PVDF is hindered by PMMA addition. It is well in agreement with the fact that PMMA addition into PVDF/SAN blend can enhance the interactions between PVDF and SAN chains, leading to low crystallinity of PVDF in the ternary blends. In this work, the blend samples have the same composition of PVDF (70 wt.%) with various ratio of PMMA and SAN content. Therefore, the difference in the crystallinity of PVDF in the blends can not be so remarkable.

Contact angle test

The contact angle test was carried out on the smooth surface of the blend samples. The hydrophilicity of PVDF/SAN (70/30) is affected by PMMA addition in blends. The contact angles against two liquids are listed in Table 4, while the surface tension and the components of surface tension are calculated by the device through the application of the Owens–Wendt approach [24], as reported in our previous work [15, 16].

Table 4 Contact angles of distilled water and diiodomethane, and solid surface tensions γ_s (including components γ_s^d and γ_s^p)

Surface	Contact angle (°)		Surface		tensions
	Distilled water	Diiodomethane	γ_s	γ_s^d	γ_s^p
PVDF/PMMA/SAN blends					
70/0/30	82.7	28.4	45.31	42.37	2.95
70/9/21	81.7	27.5	45.75	42.53	3.22
70/15/15	78.5	26.4	46.66	42.35	4.31
70/21/9	78.4	25.9	46.84	42.51	4.33
70/30/0	77.1	25.8	47.11	42.30	4.82
SAN	75.9	24.2	47.87	42.67	5.20
PMMA	71.6	21.3	49.78	42.82	6.92

It has been demonstrated that the lower the contact angle against water, the more hydrophilic the sample is [16, 44]. In Table 4, the contact angles against water decrease as the PMMA weight fraction increased. This indicates that the PMMA addition increases the hydrophilicity of the PVDF/SAN (70/30) blend. Hence, a more hydrophilic PVDF/SAN blend can be prepared by incorporating PMMA. As the PMMA content is increased to 15 wt.% in the ternary blend, the contact angle is decreased from 82.7° (PVDF/SAN binary blend) to 78.5°. When more PMMA is added into PVDF/SAN (70/30) blend (>15 wt.%), the water contact angle changes a little. Therefore, in order to obtain the hydrophilic PVDF/PMMA/SAN blend (70 wt.% PVDF), 15 wt.% PMMA is sufficient in the blend.

By proceeding with the contact angle test through two liquids (water and diiodomethane), the total surface tension γ_s, which consists of the two components of dispersive part γ_s^d and polar part γ_s^p [24]. The detailed results are given in Table 4. The total surface tension γ_s of SAN and PMMA are 47.87, and 49.78 mJ/m^2, respectively. The difference in total surface tension between these two polymers can be assigned to the different contributions of functional groups in their chains. Among those blend polymers listed in Table 4, the PMMA sample has the lowest water contact angle and the highest total surface tension. As illustrated in Fig. 6, each sample has a close value to the dispersive part of the surface tension. This implies that the polar component plays the main role in contributions to the surface tension when varying PMMA/SAN composition in the blend (70 wt.% PVDF). It is obvious that when the mass ratio PVDF/PMMA/SAN=70/15/15, both dispersive

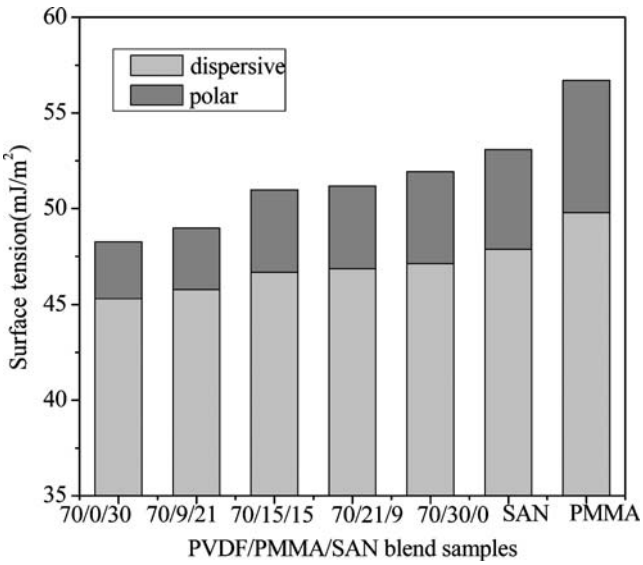

Fig. 6 The surface tension including dispersive and polar component as a function of PMMA contents in the samples

and polar parts of the surface tension increase a little. This agrees with the result of water contact angle.

Conclusions

This work confirmed that partially miscible PVDF/SAN polymer blends could be compatibilized by addition of a third polymer, PMMA. As illustrated by SEM, the required amount of PMMA is no more than 15 wt.% in the ternary blends which containing 70 wt.% PVDF, in which a more regular and homogeneous morphology was obtained. The IR and DSC results show that the interactions between polymer chains were enhanced with PMMA content increased in the PVDF/PMMA/SAN blend. The remarkable melting point depression in the ternary blend was indicated that the interactions between each component were enhanced, leading to significant obstruction of PVDF crystallization. As demonstrated by IR and WAXD measurements, only α phase regardless of PMMA content in the blend.

On the other hand, the hydrophilicity of PVDF/SAN (70 wt.% PVDF) can be further improved by adding PMMA. Through contact angle test and calculation of surface tension of the blend surface, the total surface tension increased with PMMA addition because of the increased of the polar component contribution. As the PMMA content reached 15 wt.%, the stable hydrophilicity was obtained. Therefore, this observation is a positive evidence for the blend compatibilization, which indicates that PMMA is an ideal compatibilizer for PVDF/SAN blend to prepare more homogenous and hydrophilic polymer blend.

Acknowledgment Financial support from the Key Project of BMSTC (D0406003040191) is gratefully acknowledged.

References

1. Feldman D (2005) J Macromol Sci A, Pure Appl Chem 42:587
2. Wang TT, Nishi T (1977) Macromolecules 10:421
3. Linares A, Acosta JL (1998) J Appl Polym Sci 67:997
4. Gupta AK, Bajpai R, Keller JM (2006) J Mater Sci 41:5857
5. Chui HJ (2002) J Polym Res-Taiwan 9:169
6. Chen NP, Hong L (2002) Polymer 43:1429
7. Liu JP, Jungnickel BJ (2003) J Polym Sci Part B, Polym Phys 41:873
8. Alfonso GC, Turturro A, Pizzoli M, Scandola M, Ceccorulli G (1989) J Polym Sc B, Polym Phys 27:1195
9. Li SH, Woo EM, Weak (2008) J Appl Polym Sci 107:766
10. Nunes SP, Peinemann KV (1992) J Membr Sci 73:25
11. Yang MC, Liu TY (2003) J Membr Sci 226:119
12. Moussaif N, Jerome R (1999) Polymer 40:3919
13. Classen S, Vogt M, Wendorff JH (1995) Polym Adv Technol 6:616
14. Kim KJ, Cho HW, Yoon KJ (2003) Eur Polym J 39:1249
15. Ma W, Zhang J, Chen S, Wang X (2008) Colloid Polym Sci 286:1193
16. Ma W, Zhang J, Wang X, Wang S (2007) Appl Surf Sci 253:8377
17. Kumaraswamy GN, Ranganathaiah C, Deepa Urs MV, Ravikumar HB (2006) Eur Polym J 42:2655
18. Suryanarayana C, Grant NM (1998) X-ray diffraction: a practical approach. Plenum, New York
19. Ma W, Zhang J, Wang X (2007) Appl Surf Sci 254:2947
20. Gu M, Zhang J, Wang X, Ma W (2006) J Appl Polym Sci 102:3714
21. Tao H, Zhang J, Wang X, Gao J (2007) J Polym Sci B, Polym Phys 45:153
22. Nakawa K, Ishida Y (1973) J Polym Sci, Polym Phys Ed 11:2153
23. Long Y, Shanks RA, Stachurski ZH (1995) Polymer 20:651
24. Owens DK, Wendt RC (1969) J Appl Polym Sci 13:1741
25. Spelt JK (1990) Colloids Surf 43:389
26. Nishi T, Wang TT (1975) Macromolecules 8:909
27. Sasaki H, Bala PK, Yoshida H, Ito E (1995) Polymer 36:4805
28. Roerdink E, Challa G (1978) Polymer 19:173
29. Kobayashi M, Tashiro K, Tadokoro H (1975) Macromolecules 8:158
30. Gregorio Jr R (2006) J Appl Polym Sci 100:3272
31. Gregorio Jr R, Nociti NCPS (1995) J Phys D, Appl Phys 28:432
32. Sun YP, Lawson GE, Bunker CE, Johnson RA, Ma B, Farmer C, Riggs JE, Kitaygorodskiy A (1996) Macromolecules 29:8441
33. Benedetti E, Catanorchi S, D'Alessio A, Vergamini P, Ciardelli F, Pracella M (1998) Polym Int 45:373
34. Davis GT, McKinney JE, Broadhurst MG, Roth SC (1978) J Appl Phys 49:4998
35. Gregorio Jr R, Cestari M (1994) J Polym Sci B, Polym Phys 32:859
36. Hodge RM, Edward GH, Simon GP (1996) Polymer 3:1371
37. Martuscelli E, Canetti M, Vicini L, Seves A (1982) Polymer 23:331
38. Lim GBA, Lloyd DR (1993) Polym Eng Sci 33:529
39. Kim SS, Lloyd DR (1992) Polymer 33:1036
40. Beck HN, Ledbetter HD (1965) J Appl Polym Sci 9:2131
41. Pillin I, Pimbert S, Levesque G (2002) Polym Eng Sci 42:2193
42. Wang J, Dou Q, Wu S, Chen X (2007) Polym Eng Sci 47:889
43. Kumar SK, Colby RH, Anastasiadis SH, Fytas G (1996) J Chem Phys 105:3777
44. Huang C, Zhang L (2004) J Appl Polym Sci 92:1